Available online at www.sciencedirect.com

ScienceDirect

Energy Procedia 161 (2019) 403–411

Energy Procedia

www.elsevier.com/locate/procedia

2nd International Conference on Sustainable Energy and Resource Use in Food Chains, ICSEF 2018, 17-19 October 2019, Paphos, Cyprus

An investigation into sCO_2 compressor performance prediction in the supercritical region for power systems

Samira Sayad Saravi*, Savvas A. Tassou

Brunel University London, Institute of Energy Futures, Centre for Sustainable Energy use in Food chains (CSEF), Uxbridge, UB8 3PH, United Kingdom

Abstract

This paper focuses on predicting centrifugal compressor performance in the supercritical region of real gas. For this purpose, thermodynamic changes have been considered in the sub-regions of the supercritical space. It is known that some properties (e.g. compressibility or density) of supercritical fluids behave anomalously in a narrow temperature-pressure band, shaped by pseudocritical lines, which start at the critical point and extend to higher T and P values. To accurately predict the performance of supercritical carbon dioxide (sCO_2) turbomachinery, the fluid behavior, in three regions (liquid-like, pseudocritical and vapour-like) created by pseudocritical lines, should be considered. For this purpose, computational fluid dynamics (CFD) is employed to calculate compressor performance in different regions of the supercritical space. The selected compressor geometry is the compressor impeller tested in the Sandia sCO_2 compression loop facility. The results illustrate that operating points in the liquid-like region achieve the highest pressure rise. In addition, fluctuations in two fluid properties, density and speed of sound, have been observed wherever their pseudocritical lines have been crossed. However, the reason for these variations needs more investigation. The study considers the sudden changes occurring in the supercritical region and should lead to more accurate prediction of compressor performance,.

Keywords: supercritical CO_2; turbomachinary desing; computational fluid dynamics; real gas thermodynamics

* Corresponding author. Tel.: +44-1895-267707; fax: +44-1895-269777.
E-mail address: samira.sayadsaravi@brunel.ac.uk

10.1016/j.egypro.2019.02.098

Nomenclature

c_s	speed of sound
κ_T	isothermal compressibility
ρ	density
M	Mach number
P	pressure
T	temperature
LL	liquid-like
PC	pseudocritical
VL	vapour-like

1. Introduction

The environmental impact of fossil fuel consumption has brought global attention to our primary sources of energy. One way of reducing energy demand is through the use of supercritical carbon dioxide (sCO_2) as a working fluid in energy conversion systems. sCO_2 power cycles can increase the thermal-to-electric conversion efficiency by up to 50% when compared with conventional gas turbines [1]. These cycles operate in a similar manner to other Joule-Brayton cycles and use carbon dioxide in its supercritical region [2]. CO_2 is a high density working fluid; this enables the design of equipment that is highly compact for the same power output, when compared to steam Rankine cycle (SRC) and organic Rankine cycle (ORC) equipment. Additionally, CO_2 is a low-cost, non-flammable and non-toxic working fluid [3]. Supercritical CO_2 systems were originally conceived for nuclear or concentrated solar power generation applications [4, 5]. However, the availability of high-temperature waste heat in industrial environments and the inability of working fluids employed in ORC systems, provided the impetus for consideration of the sCO_2 cycle for a broader range of applications, including waste heat for power generation.

To date, most of the interest and development of sCO_2 heat-to-power systems has taken place in the MWe power range for market and economic reasons and the availability of sCO_2 components from the petrochemical industry. Very little work has been carried out in the sub-100 kWe power range due to challenges of turbomachinery design and cost. Usage of sCO_2 in this power range will increase the overall thermal efficiency of these systems even at moderate turbine inlet temperatures that is existing excessively in the industrial environment and is considered as waste. There is a lack of literature on the impact of supercritical gas characteristics on compressor performance in this power range. Only two empirical studies, by Sandia National Laboratory and Tokyo Institute of Technology, have been predominantly carried out to demonstrate the feasibility of sCO_2 Brayton cycle applications and to examine the system performance and characteristics [6-8].

Compressor operation in the supercritical space causes instabilities in the compressor performance that need to be addressed through the design process [6]. For instance, a slight change in the temperature can create a fluctuation in the gas properties, affecting the operation. These changes are related to the sub-regions in supercritical space, which need to be well-known before the start of the design process.

In a narrow temperature-pressure (T - P) band that starts at the critical point and extends to higher T and P values, some properties of the sCO_2 (e.g. compressibility or density) may behave anomalously [9-13]. These anomalies can be identified in pressure-temperature space by curves signifying inflection points of the relevant thermodynamic properties; these curves, as a group, are named pseudocritical lines (PC lines), or Widom lines [14]. Different physicochemical quantities (e.g. compressibility, heat capacity, density and speed of sound) have different PC lines and collectively these curves define a pseudocritical region, located in a wedge-shaped area [12, 15 and 16].

Fig. 1 illustrates the CO_2 phase diagram in P-T projection, calculated with the Wagner-Span equation of state (EOS) [17]. In this figure, the supercritical region has been divided into three areas: liquid-like (LL), pseudocritical (PC) and vapour-like (VL) regions. The stable and metastable regions are demonstrated in Fig. 1. The approximate location of the metastable regions need to be mentioned here because the pseudocritical lines can be regarded as their ‘‘shadows’’ cast beyond the critical point [12].

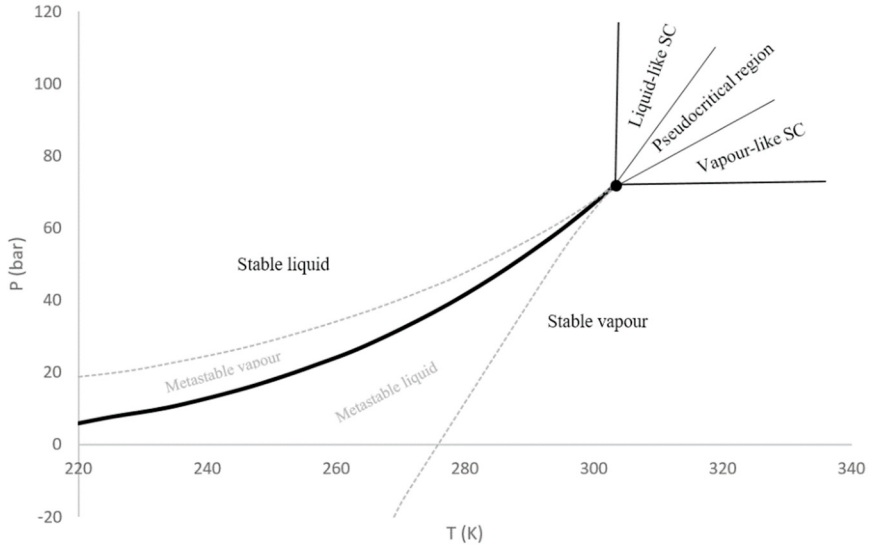

Fig. 1. Phase diagram of CO_2 showing the defined supercritical regions: liquid-like, the pseudocritical and vapour-like. In the subcritical region, stable and metastable phases (grey dot-dashed) are demonstrated [12].

2. Scope and approach

While a great deal of work has been carried out on characterizing and modelling thermodynamic real gas state, very little is known about the effects of sub-regions of supercritical space on the behavior of sCO_2 in fluid machinery. Some studies show that the uncertainty of the estimation of the compressibility, heat capacity or density is high [18]. Knowledge of the location of this anomalous region is therefore crucial when predicting the compressor operation and is necessary in order to give designers an awareness of the P-T conditions that should be taken into account. The aim of this paper is to rigorously characterize the impact of PC lines' locations in supercritical space on turbomachinery performance. In order to achieve this, first the sCO_2 sub-regions and PC lines and their effects on turbomachinery performance are to be characterized; next, the real gas effects on the internal flow behavior in three defined sub-regions is quantified. The performance of a centrifugal compressor is assessed under different conditions using computational fluid dynamics (CFD) calculations. The designed compressor has the dimensions of the SNL compressor (Table 1). Finally, the impact of PC lines on stage performance is investigated. It will be shown that, in supercritical space, variations in regions can significantly impact the compressor performance.

Table 1. Compressor design features and its comparison with TiTech (2011) and SNL (2010) compressors.

Model	TiTech	SNL	Present study
Impeller exit diameter (mm)	76	37.3	37.3
Impeller-tip inlet diameter (mm)	40	18.7	18.7
Impeller-hub inlet diameter (mm)	19.97	5.1	5.1
Outflow depth (mm)	3.42	1.7	1.7
Clearance gap (mm)	0.20	0.25	0.25
Number of impeller blades	16	6/6	6/6

3. Effect of sub-regions in supercritical space on compressor performance

Three CO_2 properties have been selected for investigation into the effect of the anomalous behavior of these properties on compressor performance. The reason for this selection is that these three properties determine the boundary of the PC region, with the other properties' anomalous lines falling inside this region. The isothermal compressibility, κ_T, is infinite at the critical point. The PC line of the compressibility is the locus of κ_T maxima on the P-T plane, with κ_T becoming higher and sharper as the critical point is approached. The speed of sound, c_s, becomes zero at the critical point; and its PC line is the location of the nonzero minimums in the supercritical region.

The density PC line has inflection and is a locus of maximum gradient points of the density, ρ. For instance, a 0.1MPa pressure drop (from 77.5bar to 76.5bar) can cause a density drop of more than 25% at temperature 306K. Similarly, a 2K temperature drop (from 305.5K to 303.2K) can induce a density increase of approximately 17% at pressure 7.6MPa.

Fig. 2 shows the PC lines for κ_T, c_s and ρ plotted up to three times critical pressure, from the critical point to about 400K and 200bar. The PC lines, in this figure, are approximated by cubic polynomials from the Wagner-Span reference EOS [12].

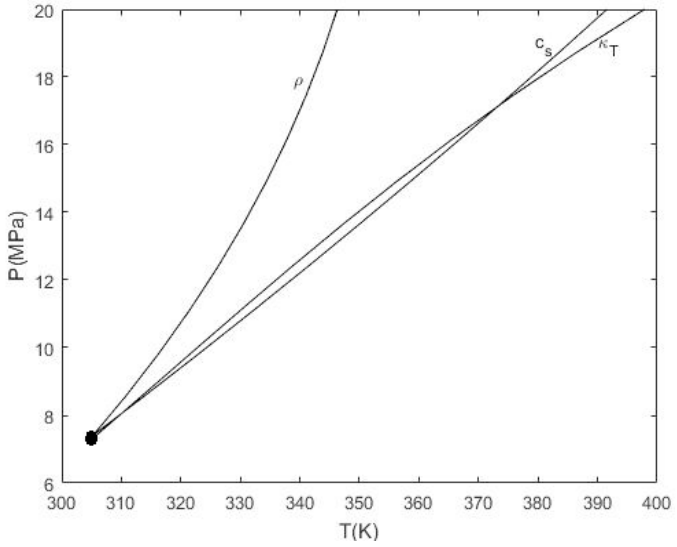

Fig. 2. The pseudocritical zone is bounded by the PC lines of the isothermal compressibility (κ_T) and speed of sound (c_s) from the high-temperature side, while on the low-temperature side it is limited by the PC line of the density (ρ) [12].

The abrupt changes related to these lines require particular attention; these changes would affect compressor performance under different performance conditions. Utamuraa et al. (2012) [8] have reported that in the vapour-like region, the pressure ratio has been overestimated by their prediction, when compared to their experimental data.

Compressor performance test data by TiTech and SNL has also been considered in this study. TiTech's experimental results show that most of the inlet and outlet performance conditions are located in the vapour-like region. The maximum design conditions of the test apparatus was selected to be 11MPa pressure, 150°C temperature, a 6kg/s flow rate and a rotation rate of 24,000rpm. Different compressor design points were examined with three different impeller dimensions. They claimed that there was no unstable phenomena in the area where the CO_2 properties change sharply [19].

In the SNL experiment, the compressor inlet conditions varied from 304.3-307K and 7700-8139kPa. They compared the measured values with the predicted performance for shaft speeds between 45,000rpm and 65,000rpm. The map for corrected enthalpy and corrected mass flow shows good agreement [6, 20].

Both of the above experiments chose to investigate various pressure and temperature inlet conditions; however, there is still a need to select specific conditions to compare the performance in different sub-regions. This study has therefore considered a range of boundary conditions, selected to enable identification of the effect of PC lines on the stage performance. The next section details the modelling setup for performance prediction.

4. Modelling setup

Simulations were carried out for six initial conditions in different supercritical sub-regions. Inlet conditions in the 305-315K temperature range and at two pressures around 8.0MPa and 9.0MPa were chosen. The corresponding shaft speed is constant and is considered to be 55,000rpm in order to be comparable with Sandia existing data. Compressor inlet operating conditions were determined to avoid the formation of liquid where the flow is accelerated locally.

CFX 17.1 was employed to perform single-passage steady state calculations (see Fig. 3). The wheel's meshes were generated in ANSYS-TurboGrid. An ATM optimized topology was employed inside the impeller, with meshes approximately 10^{+6} nodes. Turbulence k-e and total energy were used for the modelling fluid, with total pressure and total temperature defined as inlet boundary conditions with flow direction normal to the boundary. Outlet average static pressure were chosen as the outlet boundary condition.

Fig. 3. Left: designed centrifugal compressor and its flow path, in green, for CFD modelling; Middle: the SNL compressor; Right: ANSYS-TurboGrid Mesh.

To simulate the real gas effect, the Span-Wagner EOS model was used as the recommended model to accurately generate the flow properties [21]. For this purpose, an RGP (real gas property) format table was created to implement the variable properties in the CFX code. The user-defined table includes CO_2 features such as specific heat ratio and density near the critical point, which fluctuates due to the phase change effect. These characteristics are created by the NIST REFPROP 8.0 fluid property database. The generated properties files have been combined with a MATLAB code to create a lookup table as an input of TASCflow RGP in ANSYS CFX 17.1.

5. Results

The inlet and outlet conditions for each operating point are detailed in Tables 2 and 3. Two inlet pressure conditions (80bar and 90bar) with different inlet temperatures have been studied for a constant compressor shaft speed of 55,000rpm in all cases.

In Table 2, the pressure ratio for model 80M2 shows 14% increase in the liquid-like region compared to the vapour-like region; this pressure ratio increase occurs for only a 1.4% decrease in the inlet temperature. The pressure ratio in the PC and VL regions are very similar, but the PC region is slightly higher.

Table 2. Comparison of results for different operating points at 55,000rpm with approximately 80bar inlet pressure.

Operation conditions	80M1	80M2	80M3
Inlet pressure (bar)	79.50	79.85	81.93
Inlet temperature (K)	308.02	306.38	310.69
Outlet pressure (bar)	102.99	116.83	102.67
Outlet temperature (k)	320.47	320.45	323.18
Pressure ratio	1.29	1.46	1.25
Region (inlet/outlet)	PC/PC	LL/LL	VL/PC

Table 3. Comparison of results for different operating points at 55,000rpm with approximately 90bar inlet pressure.

Operation conditions	90M1	90M2	90M3
Inlet pressure (bar)	87.54	89.42	90.29
Inlet temperature (K)	310.54	313.72	316.4
Outlet pressure (bar)	110.09	111.48	111.28
Outlet temperature (k)	319.30	324.83	328.47
Pressure ratio	1.25	1.24	1.23
Region (inlet/outlet)	LL/LL	PC/PC	VL/PC

Fig. 4 also presents the results in the supercritical space. It demonstrates the inlet and the outlet conditions in different sub-regions. For instance, models 80M3 and 90M3 have the inlet condition in the VL space, but the outlet is located on the PC region. This consideration would add to the challenges of the performance prediction. Not only should the inlet condition be carefully selected, but the outlet results also need to be predicted accurately. In particular, the outcome of this compression would affect the system's downstream performance since crossing the PC lines would create abrupt changes in the CO_2 properties.

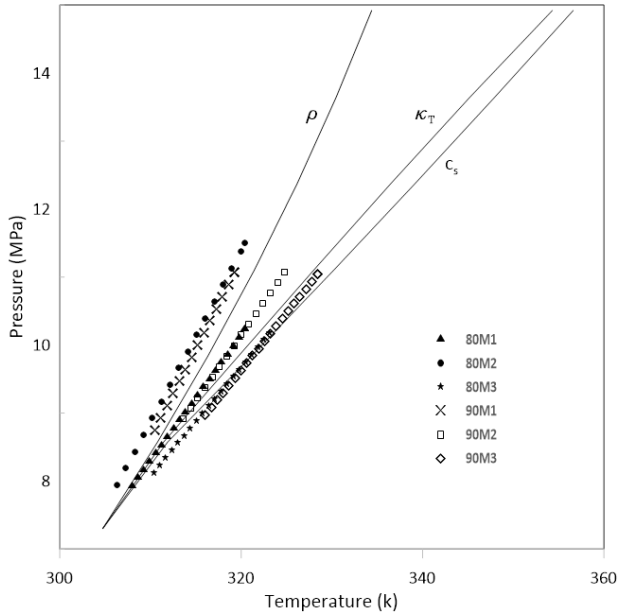

Fig. 4. Plot of compressor performance in different sub-regions of supercritical space; κ_T: isothermal compressibility, c_s: speed of sound and ρ: density.

The non-ideal fluid state gives rise to a set of derived properties that impact the governing equations of compressible flow for real gas. Studying the behavior of these properties can help identify various real gas phenomena and provide insight into the operation of a compressor stage [21]. One such property is density. Fig. 5 and Fig. 6 show the density changes inside the flow path from the inlet to the outlet in the streamline location (S/C). As is demonstrated in Fig. 4, model 80M1's P-T characteristic coincides with the density PC line. This event can be confirmed by the fluctuations observed in Fig. 5. However, the reason for this sudden change needs more investigation. In addition, models 80M2 and 90M1 both reached the highest density in following figures. The reason for this increase, compared to the other models, can be explained by their location on the supercritical space as shown in Fig. 4. Both of these models have been placed in the liquid-like region, located at the low-temperature side of the density PC line, with the PC line of this property forming the locus of density maxima on the P-T plane.

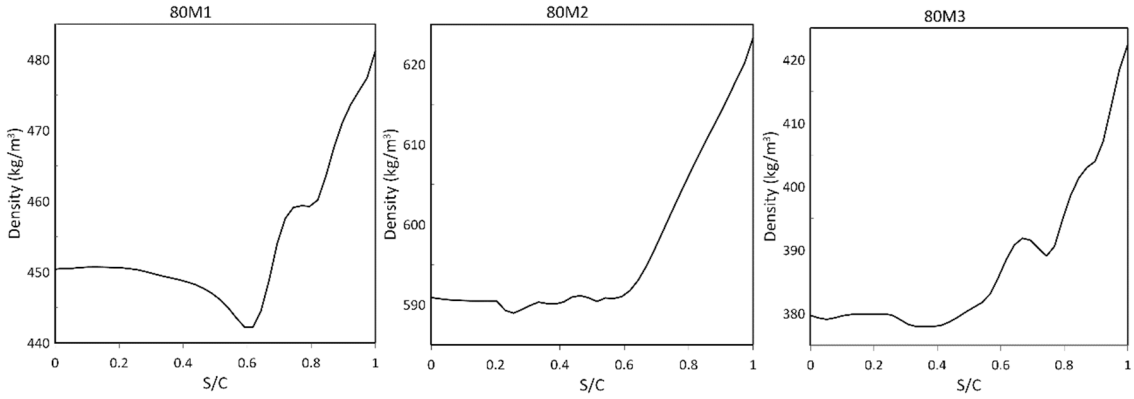

Fig. 5. Blade surface distribution of density in streamline location for models with approximately 80bar inlet pressure.

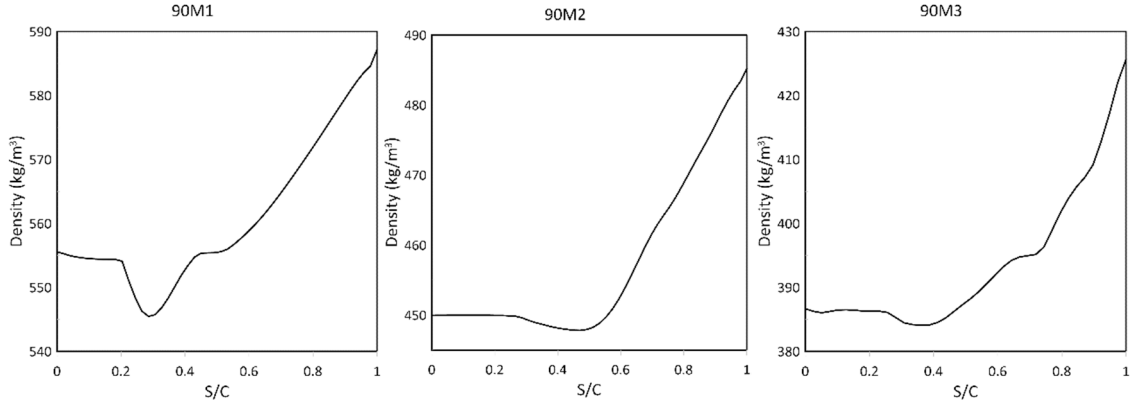

Fig. 6. Blade surface distribution of density in streamline location for models with approximately 90 bar inlet pressure.

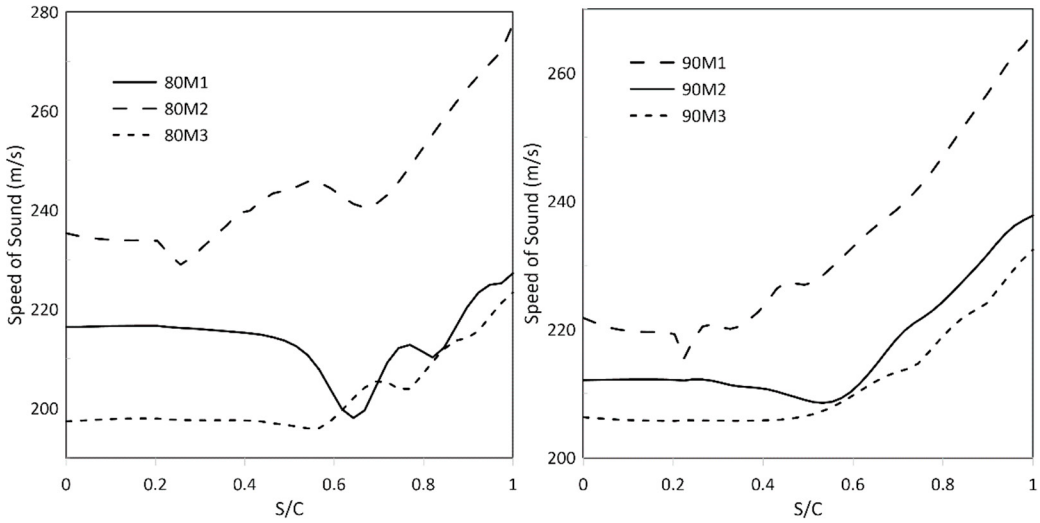

Fig. 7. Blade surface distribution of speed of sound in streamline location.

Another deviation from ideal gas theory is observed in the expression for the speed of sound of a real gas. Fig. 7 shows that the variation in the speed of sound is greater than that of the other two parameters. Among all the case studies, the maximum observed discrepancy of the speed of sound PC line belongs to the 80M3 case, which crosses the speed of sound PC line in Fig. 4. Similarly, the model 90M3 reached the lowest speed of sound, which can be confirmed by the results demonstrated in Fig. 4.

The results of the isothermal compressibility did not show fluctuations in this study. However, it is observed that models 90M3, 90M2 and 80M3 gained the maximum increase in isothermal compressibility. This finding is similar to the above results and indicates the effect of PC lines in sCO_2 turbomachinery.

6. Conclusions

This investigation presents a comprehensive assessment of sCO_2 compressor performance in the supercritical region. To account for real gas effects on stage operation, CO_2 behaviour in the supercritical space should be considered.

In a specific region, the properties of supercritical CO_2 change dramatically along supercritical P–T paths. These anomalies can be identified in the pressure–temperature space by curves that signify points of inflection of the relevant thermodynamic properties; these curves, as a group, are named pseudocritical lines. Different physicochemical quantities (e.g. compressibility, density and speed of sound) have different PC lines; collectively, these curves compose a pseudocritical region, located in a wedge-shaped area. This area divides the supercritical space into three zones: the liquid-like, pseudocritical and vapour-like regions [12].

In this paper, the variation of the sCO_2 properties projected by supercritical sub-regions are identified as the possible reason for pressure ratio increase. The changes in the density and speed of sound have been examined by changing the location of the operating points. The primary consideration was to quantitatively identify physicochemical behavior in the different supercritical regions.

CFD calculations have been used to study the wheel's internal flow when operating in different supercritical sub-regions. The flow modelling on a selected compressor was performed with ANSYS CFX 17.1, including a generated lookup table from REFPROP for CO_2 real gas properties. The compressor dimensions are the compressor impeller tested in the Sandia sCO_2 compression loop facility, which is a relatively small component with diameter of 37.3mm with 6+6 vanes. Comparisons of the results of the CFD analysis show a greater rise in pressure ratio inside the liquid-like region than in the other two areas. The second pressure increase occurs in the pseudocritical region. The vapour-like region shows the lowest pressure rise among all the zones. It can therefore be suggested that selecting a target

operational point in the liquid-like region would lead to higher pressure rise. Further investigation could consider the effect of three supercritical sub-regions in order to improve the accuracy of the performance map prediction.

Acknowledgements

The research presented in this paper has received funding from the European Union's Horizon 2020 research and innovation programme under grant agreement No. 680599. Aspects of the work are also funded by: i) the Centre for Sustainable Energy Use in Food Chains (CSEF) and, ii) the Engineering and Physical Sciences Research Council (EPSRC) funded project 'Optimising Energy Management in Industry-OPTEMIN' Grant No: EP/P04636/1. CSEF is an End Use Energy Demand Centre funded by the Research Councils UK, Grant No: EP/K011820/1. The manuscript reports all the relevant data to support the understanding of the results. More detailed information and data, if required, can be obtained by contacting the corresponding author of the paper.

References

[1] Wright, S. "Overview of S-CO_2 Power Cycles," *Mech. Eng.* 134(1) (2012): 40–43.
[2] Crespi, F., Gavagnin, G., Sánchez, D., and Martínez, G. S. "Supercritical carbon dioxide cycles for power generation: A review," *Appl. Energy* 195 (2017): 152–183.
[3] Kulhanek, M., and Dostal, V. "Supercritical carbon dioxide cycles thermodynamic analysis and comparison," Supercritical CO_2 Power Cycle Symposium, Boulder, Colorado, May (2011): 24–25.
[4] Ahn, Y., Bae, S. J., Kim, M., Cho, S. K., Baik, S., Lee, J. I., and Cha, J. E. "Review of supercritical CO_2 power cycle technology and current status of research and development," *Nuclear Engineering and Technology* 47(6) (2015): 647–661.
[5] Li, M., Wang, J., Li, S., Wang, X., He, W., and Dai, Y. "Thermo-economic analysis and comparison of a CO_2 transcritical power cycle and an organic Rankine cycle," *Geothermics* 50 (2014): 101–111.
[6] Wright, S., Radel, R., Vernon, M., Rochau, G., and Pickard, P. "Operation and Analysis of a Supercritical CO_2 Brayton Cycle," *Sandia National Laboratories*, (2010) Albuquerque, NM, Technical Report No. SAND2010-0171.
[7] Fuller, R. L., and Eisemann, K. "Centrifugal Compressor Off-Design Performance for Super-Critical CO_2," *Supercritical CO_2 Power Cycle Symposium*, Boulder, Colorado, May (2011): 24–25.
[8] Utamura, M., Fukuda, T. and Aritomi, M. "Aerodynamic Characteristics of a Centrifugal Compressor Working in Supercritical Carbon Dioxide," *2nd International Conference on Advances in Energy Engineering* (ICAEE 2011), Energy Procedia (2012): 1149–1155.
[9] Wang, Z., and Nur, A. "Effect of CO_2 flooding on wave velocities in rocks with hydrocarbons," *SPE Reservoir Engineering* 4(4) (1989): 429–436.
[10] Estrada-Alexanders, A. F., and Trusler, J. P. M. "Speed of sound in carbon dioxide at temperatures between (220 and 450) K and pressures up to 14 MPa," *J. Chem. Thermodyn.* 30(12) (1998): 1589–1601.
[11] Oschwald, M., Smith, J. J., Branam, R., Hussong, J., Schik, A., Chehroudi, B., and Talley, D. "Injection of fluids into supercritical environments," *Combust. Sci. Technol.* 178 (2006): 49–100.
[12] Imre, A. R., Ramboz, C., Deiters, U. K., and Kraska, T. "Anomalous fluid properties of carbon dioxide in the supercritical region: application to geological CO_2 storage and related hazards," *Environ Earth Sci.* 73 (2015): 4373–4384.
[13] Simeoni, G. G., Bryk, T., Gorelli, F.A., Krisch, M., Ruocco, G., Santoro, M., and Scopigno, T. "The Widom line as the crossover between liquid-like and gas-like behaviour in supercritical fluids," *Nature Phys.* 6 (2010): 503–507.
[14] Xu, L., Kumar, P., Buldyrev, S. V., Chen, S. H., Poole, P. H., Sciortino, F., and Stanley, H. E. "Relation between the Widom line and the dynamic crossover in systems with a liquid–liquid phase transition," *Proc. Natl. Acad. Sci. U.S.A.* (2005) 102: 16558–16562.
[15] Brazhkin, V. V., and Ryzhov, V. N. "Van der Waals supercritical fluid: exact formulas for special lines," *J. Chem. Phys.* 135 (2011): 084503.
[16] May, H. O., and Mausbach, P. "Riemannian geometry study of vapor–liquid phase equilibria and supercritical behavior of the Lennard-Jones fluid," *Phys. Rev. E.* 85(3) (2012): 031201.
[17] Span, R., and Wagner, W. "A New Equation of State for Carbon Dioxide Covering the Fluid Region From the Triple-Point Temperature to 1100 K at Pressures up to 800 MPa," *J. Phys. Chem.* 25(6) (1994): 1509–1596.
[18] Imre, A. R., and Tiselj, I. "Reduction of fluid property errors of various thermohydraulic codes for supercritical water systems," *Kerntechnik* 77 (2012): 18–24.
[19] Aritomi, M., Ishizuka, T., Muto, Y., and Tsuzuki, N. "Performance Test Results of a Supercritical CO_2 Compressor Used in a New Gas Turbine Generating System," *Journal of Power and Energy Systems* 5(1) (2011): 45–59.
[20] Radel, R., Conboy, T., and Wright, S. "Supercritical CO_2 Compression Loop Operation at Off-Nominal Conditions," *Sandia National Laboratories*, (2010) Albuquerque, NM, Technical Report No. SAND2010-7847C.
[21] Baltadjiev, N. D., Lettieri, C., and Spakovszky, Z. S., 2015, "An Investigation of Real Gas Effects in Supercritical CO_2 Centrifugal Compressors," *J. Turbomach*. 137 (2015): 091003(1–13).